Chemistry & Biology
Article

Hoiamide A, a Sodium Channel Activator of Unusual Architecture from a Consortium of Two Papua New Guinea Cyanobacteria

Alban Pereira,[1,3] Zhengyu Cao,[2,3] Thomas F. Murray,[2] and William H. Gerwick[1,*]
[1]Center for Marine Biotechnology and Biomedicine, Scripps Institution of Oceanography, and Skaggs School of Pharmacy and Pharmaceutical Sciences, University of California, San Diego, La Jolla, CA 92093, USA
[2]Department of Pharmacology, School of Medicine, Creighton University, Omaha, NE 68178, USA
[3]These authors contributed equally to this work
*Correspondence: wgerwick@ucsd.edu
DOI 10.1016/j.chembiol.2009.06.012

SUMMARY

Hoiamide A, a novel bioactive cyclic depsipeptide, was isolated from an environmental assemblage of the marine cyanobacteria *Lyngbya majuscula* and *Phormidium gracile* collected in Papua New Guinea. This stereochemically complex metabolite possesses a highly unusual structure, which likely derives from a mixed peptide-polyketide biogenetic origin, and includes a peptidic section featuring an acetate extended and S-adenosyl methionine modified isoleucine moiety, a triheterocyclic fragment bearing two α-methylated thiazolines and one thiazole, and a highly oxygenated and methylated C15-polyketide substructure. Pure hoiamide A potently inhibited [^{3}H]batrachotoxin binding to voltage-gated sodium channels (IC_{50} = 92.8 nM), activated sodium influx (EC_{50} = 2.31 μM) in mouse neocortical neurons, and exhibited modest cytotoxicity to cancer cells. Further investigation revealed that hoiamide A is a partial agonist of site 2 on the voltage-gated sodium channel.

INTRODUCTION

For more than 30 years, cyanobacteria, or blue-green algae, have shown an exceptional capacity to produce structurally diverse and highly bioactive secondary metabolites (Tidgewell et al., 2009). Although chemical investigations of freshwater species occurred as early as the 1930s (Fitch et al., 1934), it was the late Richard E. Moore who pioneered the chemical and biosynthetic exploration of marine cyanobacteria, beginning in 1977 with his report on majusculamides A and B (Marner et al., 1977). The continuing interest in the natural products of marine cyanobacteria is reflected in the rich literature, which has reported more than 678 compounds from these organisms, many of which possess biomedically relevant properties (Tidgewell et al., 2009). Indeed, numerous reviews of the chemistry (Tan, 2007; Van Wagoner et al., 2007; Sivonen and Borner, 2008), biological properties (Grindberg et al., 2008; Ersmark et al., 2008; Paul et al., 2007; Sielaff et al., 2006), and biosynthetic pathways (Ramaswamy et al., 2006; Moore, 2005) of marine cyanobacteria have appeared in recent years.

Among the reported bioactivities of marine cyanobacterial metabolites, a growing number of these appear to target the mammalian voltage-gated sodium channels (VGSCs), either as blockers (Wu et al., 2000; Edwards et al., 2004) or activators (Li et al., 2001). VGSCs are responsible for the rapid influx of sodium that underlies the rising phase of the action potential in electrically excitable cells, including neurons (Catterall et al., 2007). They are composed of voltage-sensing and pore-forming elements in a single protein complex of one principal α subunit (220–260 kDa) and one or two auxiliary β subunits (33–36 kDa) (Catterall et al., 2007; Denac et al., 2000; Taylor and Meldrum, 1995). Chemical substances with activity at the VGSCs may possess therapeutic value in the treatment of epilepsy, neuropathic pain, brain damage from ischemia and certain types of stroke, as well as heart failure (Denac et al., 2000). VGSCs serve as the molecular targets for toxins that act at six or more distinct receptor sites on the channel protein (Catterall et al., 2007). They include tetrodotoxin (TTX), saxitoxin, and μ-conotoxin (neurotoxin site 1); batrachotoxin, veratridine, aconitine, and grayanotoxin (neurotoxin site 2); α-scorpion toxins and sea anemone toxins (neurotoxin site 3); β-scorpion toxins (neurotoxin site 4); brevetoxins and ciguatoxin (neurotoxin site 5); δ-conotoxin (neurotoxin site 6); DDT and pyrethoids (neurotoxin site 7); and antillatoxin (undefined receptor site) (Catterall et al., 2007; Li et al., 2001; Denac et al., 2000; Taylor and Meldrum, 1995). Currently, therapeutic uses of drugs that modulate sodium channel function include local anesthetics, antiarrythmics, anticonvulsants, and neuroprotective agents (Taylor and Meldrum, 1995). Because of their high affinity and specificity, natural product sodium channel ligands have served as important tools to explore the structure and function of VGSCs (Catterall et al., 2007).

As part of our ongoing assay-based screening program for new neuroactive compounds from cyanobacteria, we found that the extract of a Papua New Guinea consortium of two cyanobacteria, *Lyngbya majuscula* and *Phormidium gracile*, exhibited potent inhibition of calcium oscillations and activation of sodium influx in mouse cerebrocortical neurons. Additionally, modest cytotoxicity against human lung adenocarcinoma (H460) and mouse neuroblastoma (Neuro2a) cell lines was recorded for this extract. A combination of bioassay and ^{1}H nuclear magnetic

Table 1. NMR Data of Hoiamide A (1) in DMSO-d_6

Unit	Carbon	δ_C[a]	δ_H, multiplicity (Hz)[b]	COSY	HMBC (^{1}H to ^{13}C)	NOESY
Thr	1	170.2				
	2	58.0	4.55, dd (7.7, 2.8)	2NH, 3	1, 3	4
			NH 7.86, d (8.0)	2	2, 3, 5	4, 6, 7
	3	66.0	4.28, m	2, 4		
	4	20.2	1.15, d (6.6)	3	2, 3	2, 2NH
Hiva	5	169.4				
	6	75.8	4.91, d (3.4)	7	5, 7, 8, 9, 10	2NH, 8
	7	30.0	2.18, m	6, 8, 9	8	2NH
	8	18.9	0.90, d (6.9)	7	6, 7, 9	6
	9	16.0	0.76, d (6.9)	7	6, 7, 8	
Ahdhe	10	174.2				
	11	44.3	2.30, dq (9.0, 7.2)	12, 18	10, 12, 18	13NH
	12	71.1	3.78, d (9.6)	11	10, 11, 18	17, 18
	13	52.6	3.53, dd (11.4, 10.2)	13NH, 14	14, 17, 19	15a, 17, 18
			NH 6.82, d (9.8)	13	12, 13, 19	11, 14, 22
	14	35.8	1.55, m	13, 15b, 17		13NH
	15	25.1	a1.04, ddq (13.8, 7.8, 7.2)	15b, 16	13, 16, 17	13
			b1.42, m	14, 15a, 16	14	
	16	11.1	0.838, t (6.3)	15a, 15b	15	
	17	15.6	0.85, d (6.0)	14	13, 14, 15	12, 13
	18	13.8	0.95, d (6.8)	11	10, 11, 12	12, 13
MoCys1	19	173.1				
	20	84.6				
	21	41.0	a3.19, d (11.4)	21b	19, 20, 22, 23	22
			b3.81, d (11.4)	21a	19, 20, 22, 23	22
	22	25.4	1.54, s		19, 20, 21	21a, 21b, 13NH
MoCys2	23	175.8				
	24	83.3				
	25	42.6	a3.46, d (11.2)	25b	23, 24, 26, 27	26
			b3.51, d (11.0)	25a	23, 24, 26	
	26	24.1	1.63, s		23, 24, 25	25a
MoCys3	27	162.1				
	28	147.4				
	29	122.4	8.01, s		27, 28, 30	
Dmetua	30	168.3				
	31	33.1	a2.92, dd (15.8, 2.0)	31b, 32	30	34, 43
			b2.99, dd (15.8, 9.2)	31a, 32	30, 32	43
	32	79.5	3.80, m	31a, 31b, 33	30, 43, 44	43
	33	35.7	2.34, m	32, 34, 43	32, 34	35, 44
	34	75.2	5.18, d (9.8)	33, 35	1, 32, 33, 35, 36, 42	31a, 36, 43
	35	38.5	1.70, dq (7.8, 7.2)	34, 36, 42	33, 36, 42	33, 41, 43
	36	72.1	3.18, dd (10.2, 1.4)	35, 37	34, 38, 41	34, 38b, 42
	37	33.6	1.48, m	36, 38a, 38b, 41	38, 39	42
	38	36.6	a1.15, m	37, 39	36, 37, 39, 40, 41	36
			b1.26, m	37	37, 39, 40, 41	
	39	19.9	1.25, m	38a, 40	38	
	40	14.3	0.835, t (6.8)	39	39	
	41	11.9	0.72, d (6.6)	37	36, 37, 38	35
	42	10.0	0.82, d (6.8)	35	35, 36	36, 37

Table 1. *Continued*

Unit	Carbon	δ_C[a]	δ_H, multiplicity (Hz)[b]	COSY	HMBC (^{1}H to ^{13}C)	NOESY
	43	10.8	0.838, d (6.3)	33	32, 33, 34	31a, 31b, 32, 34, 35
	44	56.7	3.23, s		32	33

[a] Recorded at 125 MHz.
[b] Recorded at 500 MHz.

resonance (NMR)–guided fractionation led to the discovery of a highly unusual cyclic peptide, named hoiamide A (**1**), as the major bioactive component of the extract. Here, we describe the isolation and structure elucidation of this novel natural product, including complete stereochemistry and a detailed biological evaluation of its neuroactive properties and site of action at the mammalian VGSC.

RESULTS AND DISCUSSION

Hoiamide A: Isolation and Planar Structure Elucidation

A dark purple composite collection of two intertwined cyanobacteria, *Lyngbya majuscula* and *Phormidium gracile*, was collected by SCUBA in Hoia Bay, Papua New Guinea. The cyanobacterial collection was extracted repeatedly with CH_2Cl_2/MeOH (2:1) and was fractioned by silica gel vacuum column chromatography to produce nine fractions (A–I). Fraction F was found to be highly active in suppressing calcium oscillations in mouse neocortical neurons and was thus subjected to a ^{1}H NMR-guided fractionation composed of repetitive silica gel flash column chromatography followed by reversed-phased high-performance liquid chromatography (HPLC) to yield the new natural product hoiamide A (**1**) {$[\alpha]^{23}_D$ +5 (c 5.5, $CHCl_3$)}. Pure hoiamide A showed exceptional potency in suppressing calcium oscillations in this neuron preparation (IC_{50} = 47.5 nM).

HRESIMS of **1** yielded an $[M+H]^+$ peak at *m/z* 926.4446, with a complex isotopic pattern composed of *m/z* 926/927/928/929/930 (100:58:28:10:3 ratio), suggesting the presence of at least three sulfur atoms. Combining this information with NMR spectroscopic data (Table 1), it was possible to derive the molecular formula $C_{44}H_{70}N_5O_{10}S_3$ (calcd for $C_{44}H_{71}N_5O_{10}S_3$, 926.4441), exhibiting 12 degrees of unsaturation. Acetylation of **1** under standard conditions afforded a triacetate derivative (**2**) with an $[M+H]^+$ ion at *m/z* 1052.4743 (calcd for $C_{50}H_{78}N_5O_{13}S_3$, 1052.4758), suggesting the presence of three OH groups. A ^{1}H NMR spectrum of **1** in dimethyl sulfoxide (DMSO)–d_6 (Table 1) displayed resonances characteristic of a peptide containing numerous aliphatic and oxygenated residues, including one aromatic singlet at δ8.01; two exchangeable NH peaks at δ7.86 (d, *J* = 8.0 Hz) and δ6.82 (d, *J* = 9.8 Hz); eight methines adjacent to O/N at δ5.18 (d, *J* = 9.8 Hz), δ4.91 (d, *J* = 3.4 Hz), δ4.55 (dd, *J* = 7.7, 2.8 Hz), δ4.28 (m), δ3.80 (m), δ3.78 (d, *J* = 9.6 Hz), δ3.53 (dd, *J* = 11.4, 10.2 Hz), and δ3.18 (dd, *J* = 10.2, 1.4 Hz); one methoxy group at δ3.23; and two methyl singlets at δ1.63 and δ1.54, respectively. The readily interpretable ^{1}H NMR data were completed by eight methyl doublets at δ1.15 (d, *J* = 6.6 Hz), δ0.95 (d, *J* = 6.8 Hz), δ0.90 (d, *J* = 6.9 Hz), δ0.85 (d, *J* = 6.0 Hz), δ0.838 (d, *J* = 6.3 Hz), δ0.82 (d, *J* = 6.8 Hz), δ0.76 (d, *J* = 6.9 Hz), and δ0.72 (d, *J* = 6.6 Hz), as well as two methyl triplets at δ0.838 (t, *J* = 6.3 Hz) and δ0.835 (t, *J* = 6.8 Hz). An extensive analysis by two-dimensional (2D) NMR, including heteronuclear single-quantum correlation (HSQC), heteronuclear multiple bond correlation (HMBC), correlation spectroscopy (COSY), total correlation spectroscopy (TOCSY), and nuclear overhauser effect spectroscopy (NOESY), revealed three interconnected partial structures, which constituted the entirety of hoiamide A (**1**) (Figure 1).

The peptidic fragment **I** (Figure 1) was found to be composed of threonine (C1-C4), 2-hydroxyisovaleric acid (Hiva, C5-C9), and a new C3-extended isoleucine residue (4-amino-3-hydroxy-2,5-dimethylheptanoic acid, Ahdhe, C10-C18). COSY correlations between a proton at δ3.53 (Ahdhe-H13), an exchangeable proton at δ6.82 (Ahdhe-C13-NH), and a methine proton at δ1.55 (Ahdhe-H14) suggested an additional aliphatic amino acid subunit. The high field methine proton was further coupled to protons defining a *sec*-butyl side chain, according to HMBC and TOCSY data, thus suggesting the amino acid isoleucine. However, the H13 "alpha" proton showed additional coupling to an oxygenated methine at δ3.78 (d, *J* = 9.6 Hz, Ahdhe-H12) with an associated carbon at δ71.1 (Ahdhe-C12). This latter proton signal was coupled to an upfield methine at δ2.30 (dq, *J* = 9.0, 7.2 Hz, Ahdhe-H11), which, in turn, showed COSY correlations to a methyl doublet at δ0.95 (*J* = 6.8 Hz, Ahdhe-H18). Finally, the H11 methine was shown by HMBC to be adjacent to the carbonyl at δ174.2 (Ahdhe-C10); hence, this residue was defined as a three-carbon extended isoleucine residue. Long-distance HMBC correlations between the exchangeable proton at δ7.86 (Thr-C2-NH) and carbon resonances at δ58.0 (Thr-C2), δ66.0 (Thr-C3), and δ169.4 (Hiva-C5), as well as between the α-proton at δ4.91 (Hiva-H6) and carbons at δ169.4 (Hiva-C5), δ30.0 (Hiva-C7), and δ174.2 (Ahdhe-C10), firmly established the connectivity among these three residues. Similar modifications of Ile to produce Ahdhe-like residues have been observed in several other marine natural products, such as didemnins A–E (Rinehart et al., 1988) and various dolastatins (Pettit et al., 1987; Luesch et al., 2001a). In the case of hoiamide A (**1**), the ketide-extended isoleucine is methylated at the α-carbon, likely from *S*-adenosyl methionine (SAM). This finding contrasts with the pattern of methylation seen in dolastatin 10 (see Supplemental Data available online), wherein methylation occurs on the resulting secondary alcohol at the β position (e.g., the alcohol deriving from reduction of the former Ile carbonyl group). Notably, a consequence of this alternate site of methylation in hoiamide A is the creation of an additional stereocenter in the molecule.

A second substructure in **1** (Figure 1) was initiated by HMBC correlations between a methyl singlet at δ1.54 (MoCys1-H22) and quaternary carbons at δ173.1 (MoCys1-C19) and δ84.6 (MoCys1-C20), as well as a methylene at δ41.0 (MoCys1-C21), and suggested an α-methyl substituted cysteine-type residue (MoCys: modified cysteine). The diastereotopic methylene

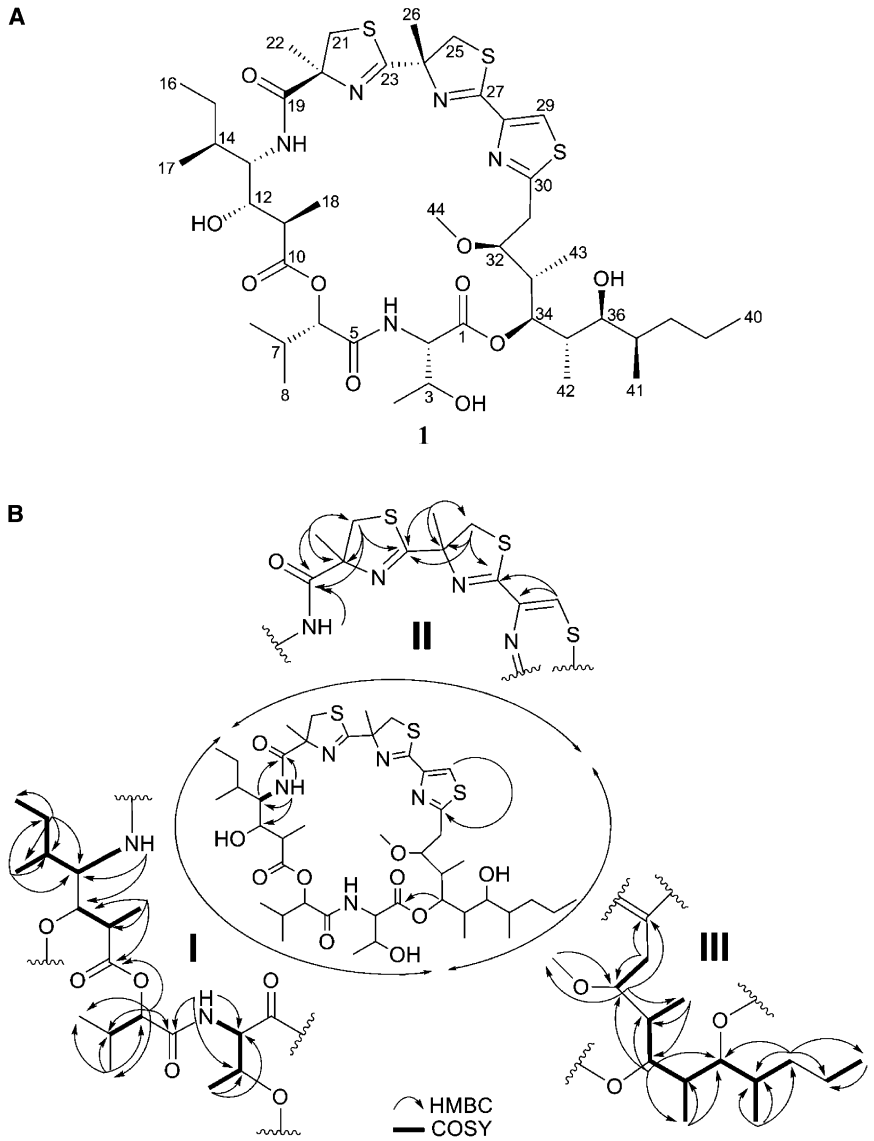

Figure 1. Structure of Hoiamide A (1)
Structure of hoiamide A (**1**) (A) and partial structures derived from NMR data (B) and their assembly by key HMBC correlations.

protons at δ3.81 (MoCys1-H21b) and δ3.19 (MoCys1-H21a), in combination with a key HMBC correlation between both H21 protons and the C23 deshielded carbon signal at δ175.8, defined this as a cyclized thiazoline. Additional HMBC correlations between the various protons of this system and all neighboring carbons two or three bonds away helped confirm these assignments (Table 1). The deshielded signal at δ175.8 (MoCys2-C23) showed HMBC correlations to a second uniquely deshielded singlet methyl group at δ1.63 (MoCys2-C26), and thus provided linkage to an additional residue. A series of ^{1}H and ^{13}C NMR signals highly comparable to those in MoCys1 were identified from HMBC data, establishing this second methyl substituted thiazoline residue (Table 1). MoCys2 was linked to a thiazole ring via tandem HMBC correlations between a deshielded quaternary carbon at δ162.1 (MoCys3-C27) and both the C25 protons and a deshielded singlet proton (δ8.01, MoCys3-H29). The two other carbon atoms of this latter residue were also identified by HMBC couplings from the lone thiazole proton and from their distinctive ^{13}C NMR shifts. A comparable arrangement of two methylated thiazolines followed by a thiazole heterocycle was first reported in the tantazole (Carmeli et al., 1990, 1993) and mirabazole (Carmeli et al., 1991) series of highly bioactive cyanobacterial metabolites, and the reported chemical shift data closely match that reported here for hoiamide A (**1**) at similar positions. Because substructure **II** was composed of two thiazolines and one thiazole, all three of which are cysteine-derived, the sulfur component of the molecular formula was fully satisfied. Finally, HMBC correlations between the protons at δ6.82 (Ahdhe-C13-NH) and δ3.53 (Ahdhe-H13) with the carbonyl resonance at δ173.1 (MoCys1-C19) provided linkage between fragments **I** and **II** in hoiamide A.

The final fragment (**III**) of hoiamide A (**1**) was determined to be a C15-polyketide (C30-C44) possessing high levels of methylation and oxygenation (Figure 1). The thiazole carbon resonance in fragment **II** at δ168.3 (Dmetua-C30) showed HMBC correlations to diastereotopic methylene protons at δ2.99 (dd, J = 15.8, 9.2 Hz, Dmetua-H31b) and δ2.92 (dd, J = 15.8, 2.0 Hz, Dmetua-H31a) (δ_C 33.1). These methylene protons showed COSY correlations to a deshielded methine proton at δ3.80 (Dmetua-H32), which, in turn, was connected by HMBC to the methyl group of a methoxy resonance as well as to another deshielded methine (δ5.18, Dmetua-H34). By ^{1}H and ^{13}C NMR chemical shift arguments, this signal was proposed to be attached to an ester, a hypothesis later verified by HMBC (see below). However, because this ester methine signal was strongly coupled to two different high field methine resonances according to COSY data, it was placed beta to the δ3.80 methine. The δ2.34 methine (Dmetua-H33) predicted to intervene between these two deshielded methines was also proton coupled to a doublet methyl, and HMBC between the δ3.80 signal and the carbon atom of this methyl group (δ10.8, Dmetua-C43) confirmed these atom relationships. The methine to the other side of the δ5.18 signal was part of a connected spin system involving sequential methylmethine, oxymethine, methylmethine, and methylene groups (Table 1). By chemical shift arguments (δ3.18, Dmetua-H36) and consideration of the molecular formula, the oxymethine at C36 was deduced to be a free secondary hydroxyl group. The latter methylene of this spin system was

connected to a terminating ethyl group by HMBC, completing partial fragment **III** as a 5,7-dihydroxy-3-methoxy-4,6,8-trimethylundecanoyl–derived residue (Dmetua). With fragments **I–III** accounting for all atoms of the molecular formula of **1** but only 11 of 12 degrees of unsaturation, it was concluded that the overall molecule formed a macrocycle. The deshielded methine at δ5.18 (Dmetua-H34) exhibited numerous HMBC cross-peaks (Figure 1), including a highly prominent three-bond correlation with an ester carbon at δ170.2 (Thr-C1), and thus established the macrocyclic planar structure of hoiamide A (**1**).

Hoiamide A: Relative and Absolute Stereochemistry

Next, we turned our attention to the absolute stereochemistry of hoiamide A (**1**). With 15 stereocenters, our initial strategy was to attempt crystallization to perform an X-ray analysis. Unfortunately, numerous efforts aimed at forming crystals from the natural product **1**, its triacetate (**2**), or the freshly prepared mono *p*-bromobenzoic ester derivative (**3**) failed to produce X-ray quality crystals. Thus, hoiamide A (**1**) was hydrolyzed with 6 N HCl (110°C, 22 hr), and the hydrolyzate was subjected to chiral HPLC, revealing the presence of (*S*)-Hiva in comparison with commercial standards. The same chromatographic technique was applied to another sample of **1**, which was first subjected to ozonolysis and oxidative workup prior to hydrolysis, and led to the detection of 2-methylcysteic acid (MCya). Comparison of retention times with freshly synthesized MCya standards (Pattenden et al., 1993; Calmes et al., 1997) confirmed the occurrence of only (*S*)-MCya. Marfey's analysis (Marfey, 1984) was performed using aliquots of the acid hydrolyzate as well as amino acid standards, employing *N*-(3-fluoro-4,6-dinitrophenyl)-L-alaninamide (L-FDAA) as the derivatizing agent, and revealed the presence of (2*S*,3*R*)-Thr in hoiamide A (**1**).

The relative stereochemistry of the C10-C18 (C3-extended Ile) and C30-C44 (Dmetua) sections was elucidated via *J*-based configuration analysis (Figure 2) (Matsumori et al., 1999). This procedure makes use of $^{3}J_{H\text{-}H}$ and $^{2\text{-}3}J_{C\text{-}H}$ values combined with nuclear Overhauser effect (NOE) and rotational nuclear Overhauser effect (ROE) data to determine the conformation of adjacent stereocenters and has been successfully applied to define the relative stereochemistry of substituted polyketides in other cyanobacterial metabolites, such as phormidolide (Williamson et al., 2002), apratoxin A (Luesch et al., 2001b), and largamide H (Plaza and Bewley, 2006). Homonuclear coupling constants were obtained from ^{1}H-NMR, E.COSY (Griesinger et al., 1987), and one-dimensional TOCSY (Uhrin and Barlow, 1997) spectra, whereas heteronuclear coupling values were accurately measured from heteronuclear long-range coupling (HETLOC) (Uhrin et al., 1998) and heteronuclear single-quantum multiple bond correlation (HSQMBC) (Williamson et al., 2000) experiments (Marquez et al., 2001). Starting with the C10-C18 section, the relative stereochemistry along C11-C12 could not be determined using *J* values alone because these did not distinguish between the two possible rotamers (*threo* **A3**, *erythro* **B3**) with H11/H12 in an anti relationship ($^{3}J_{H11\text{-}H12}$ = 9.0 Hz). Fortunately, NOESY data revealed the spatial proximity of H18 and H12, H18 and H13, as well as H11 and C13-NH, in agreement only with the *erythro* rotamer **B3**. Small homonuclear and heteronuclear *J* values were observed between C12 and C13, a result consistent only with the *threo* rotamer **A1**. The H13-H14 protons were also in an anti configuration ($^{3}J_{H13\text{-}H14}$ = 9.6 Hz); thus, NOE correlations between H13/H17, H12/H17, and H14/C13-NH confidently assigned it as rotamer **B3**.

The C30-C44 section (Dmetua) exhibited anti configurations between adjacent methines C32-C33 ($^{3}J_{H32\text{-}H33}$ = 7.9 Hz), C33-C34 ($^{3}J_{H33\text{-}H34}$ = 9.6 Hz), and C35-C36 ($^{3}J_{H35\text{-}H36}$ = 10.2 Hz), which upon analysis of key NOE correlations (H31/H43, H43/H35, and H42/H37, respectively), were assigned as *erythro* rotamers **B3**. The remaining 1,2-methine systems C34-C35 ($^{3}J_{H34\text{-}H35}$ = ~0 Hz) and C36-C37 ($^{3}J_{H36\text{-}H37}$ = ~0 Hz) were deduced to possess gauche conformations between their protons and were found to be *threo* rotamers **A1** in accordance with their heteronuclear *J* values. This proposed configuration was in agreement with all of the NOEs observed within each of the substructures.

Connection of the relative stereochemistry of the Ahdhe (C10-C18) portion with the MoCys1 residue was made possible through NOE interactions between the methine protons at δ2.30 (Ahdhe-H11) and δ1.55 (Ahdhe-H14) with the NH proton at δ6.82 (Ahdhe-C13-NH), which, in turn, was correlated with the methyl singlet at δ1.54 (MoCys1-H22) (Figure 2). Moreover, because we had established the absolute configuration of the MoCys1 residue, these observed NOEs allowed assignment of the absolute stereochemistry of Ahdhe as 11*R*, 12*S*, 13*S*, and 14*S*. Molecular modeling studies of compound **1** (Supplemental Data) confirmed that this NOE interaction was only possible with the *S* configuration at Ahdhe-C13. Thus, as with dolastatin 10, the natural configuration of Ile [e.g., L-(2*S*,3*S*)-Ile] appears to have been one of the precursors to this portion of hoiamide A (**1**).

Our initial plan for determining the absolute stereochemistry of the Dmetua substructure (C30-C44) was to form the C36 Mosher's ester derivative of compound **1**. However, this position in hoiamide A (**1**) proved to be quite resistant to acylation using Mosher's acid chloride. Instead, loss of H_2O from the Thr residue yielded the C2-C3 olefinic derivative **4** (Figure 3). Likely, steric effects disfavor reaction with the bulky α-methoxy-α-trifluoromethylphenylacetic acid (MTPA) chloride. As an alternative approach, 26 mg of the acid hydrolyzate of **1** was dissolved in MeOH/HCl and stirred at room temperature over an extended period so as to produce methyl esters of the various units composing hoiamide A (**1**). Upon solvent removal under vacuum, the residue was partitioned between EtOAc and H_2O, and both layers were subjected to extensive reversed-phase HPLC, ^{1}H-NMR, and liquid chromatography mass spectrometry (LCMS) analyses, in a search for the C10-C18 and C30-C44 sections. One such fragment, **5** {$[\alpha]^{23}_{D}$ +18 (c 0.015, MeCN)} (Figure 3), was a major component of the EtOAc fraction and displayed an M^+ at *m/z* 355.1806 consistent with the molecular formula $C_{18}H_{29}NO_4S$ (calcd 355.1812, 5 degrees of unsaturation).

The ^{1}H NMR spectrum of **5** (Table 2) showed diagnostic resonances for portions of the Dmetua substructure of **1**: a thiazole aromatic singlet at δ8.09; a methoxy singlet at δ3.95; three oxygenated methines at δ3.70 (d, *J* = 9.6 Hz), δ3.43 (dd, *J* = 10.2, 4.8 Hz), and δ2.88 (dd, *J* = 10.2, 1.8 Hz); three methyl doublets at δ0.96 (*J* = 6.6 Hz), δ0.88 (*J* = 6.0 Hz), and δ0.87 (*J* = 7.2 Hz); and one methyl triplet at δ0.79 (*J* = 7.2 Hz). Surprisingly, the singlet at δ3.95 (H18) exhibited HMBC correlations with quaternary carbon resonances at δ161.6 (C1) and δ145.6.6 (C2), indicating that this was a methyl ester at the C terminus of the

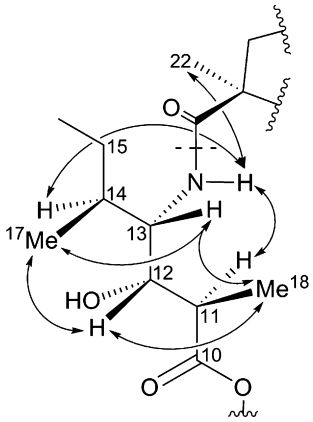

Ahdhe

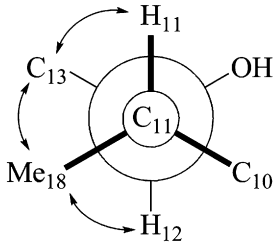

B-3[a]

$^{3}J_{H11,H12}$ = 9.0 Hz (L)
$^{3}J_{H11,C13}$ = 2.8 Hz (S)
$^{3}J_{C10,H12}$ = 0.5 Hz (S)
$^{3}J_{C18,H12}$ = 1.2 Hz (S)
$^{2}J_{H11,C12}$ =-6.5 Hz (L)

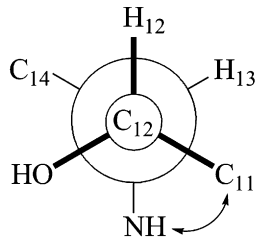

A-1[a]

$^{3}J_{H12,H13}$ = 0 Hz (S)[b]
$^{3}J_{H12,C14}$ = 0 Hz (S)[c]
$^{3}J_{C11,H13}$ = 2.6 Hz (S)
$^{2}J_{C12,H13}$ =-0.5 Hz (S)
$^{2}J_{H12,C13}$ = 0 Hz (S)[c]

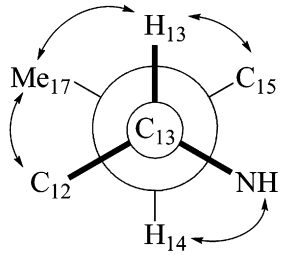

B-3[a]

$^{3}J_{H13,H14}$ = 9.6 Hz (L)
$^{3}J_{C12,H14}$ = 0 Hz (S)[c]
$^{3}J_{H13,C15}$ = 0.5 Hz (S)
$^{3}J_{H13,C17}$ = 3.9 Hz (S)
$^{2}J_{C13,H14}$ =-6.9 Hz (L)

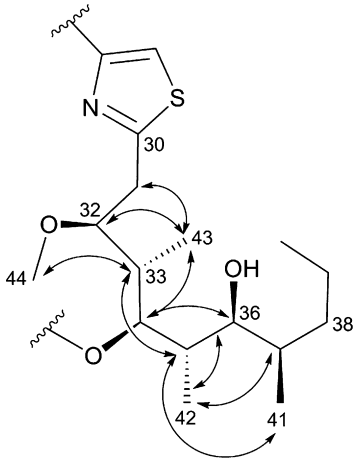

Dmetua

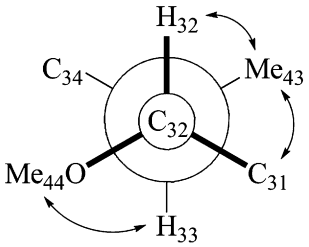

B-3[a]

$^{3}J_{H32,H33}$ = 7.9 Hz (L)
$^{3}J_{C31,H33}$ = 0 Hz (S)[c]
$^{3}J_{H32,C34}$ = 1.6 Hz (S)
$^{3}J_{H32,C43}$ = 0 Hz (S)[c]
$^{2}J_{C32,H33}$ =-6.8 Hz (L)

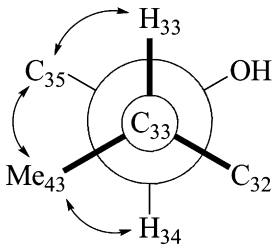

B-3[a]

$^{3}J_{H33,H34}$ = 9.6 Hz (L)
$^{3}J_{H33,C35}$ = 0 Hz (S)[c]
$^{3}J_{C32,H34}$ = 1.9 Hz (S)
$^{3}J_{C43,H34}$ = 2.4 Hz (S)
$^{2}J_{H33,C34}$ =-6.4 Hz (L)

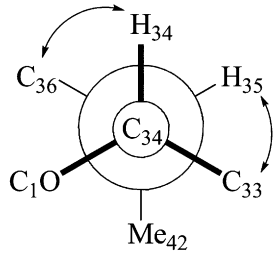

A-1[a]

$^{3}J_{H34,H35}$ = 0 Hz (S)[b]
$^{3}J_{C33,H35}$ = 0 Hz (S)[c]
$^{3}J_{H34,C36}$ = 3.1 Hz (S)
$^{3}J_{H34,C42}$ = 6.6 Hz (L)
$^{2}J_{C34,H35}$ = 0 Hz (S)[c]

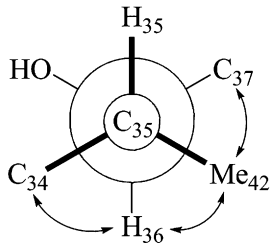

B-3[a]

$^{3}J_{H35,H36}$ =10.2 Hz (L)
$^{3}J_{H35,C37}$ = 3.1 Hz (S)
$^{3}J_{C34,H36}$ = 3.7 Hz (S)
$^{3}J_{C42,H36}$ = 0.8 Hz (S)
$^{2}J_{H35,C36}$ =-6.1 Hz (L)

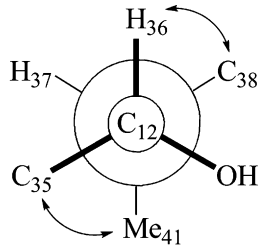

A-1[a]

$^{3}J_{H36,H37}$ = 0 Hz (S)[b]
$^{3}J_{C35,H37}$ = 0 Hz (S)[c]
$^{3}J_{H36,C38}$ = 3.6 Hz (S)
$^{3}J_{H36,C41}$ = 6.6 Hz (L)
$^{2}J_{C36,H37}$ = 0 Hz (S)[c]

↷ = NOE observed between indicated proton and proton(s) on indicated carbon

Figure 2. Homonuclear and Heteronuclear Coupling Constant Values Used to Assign the Relative Configuration of Ahdhe (C10-C18) and Dmetua (C30-C44)

The magnitude of the coupling constants, (S) for small and (L) for large, allowed identification of gauche and anti orientations between the indicated atoms. For 1,2-methine systems in which the *threo* rotamer **A3** can not be distinguished from the *erythro* rotamer **B3**, NOE data (↔) provided an unambiguous assignment.

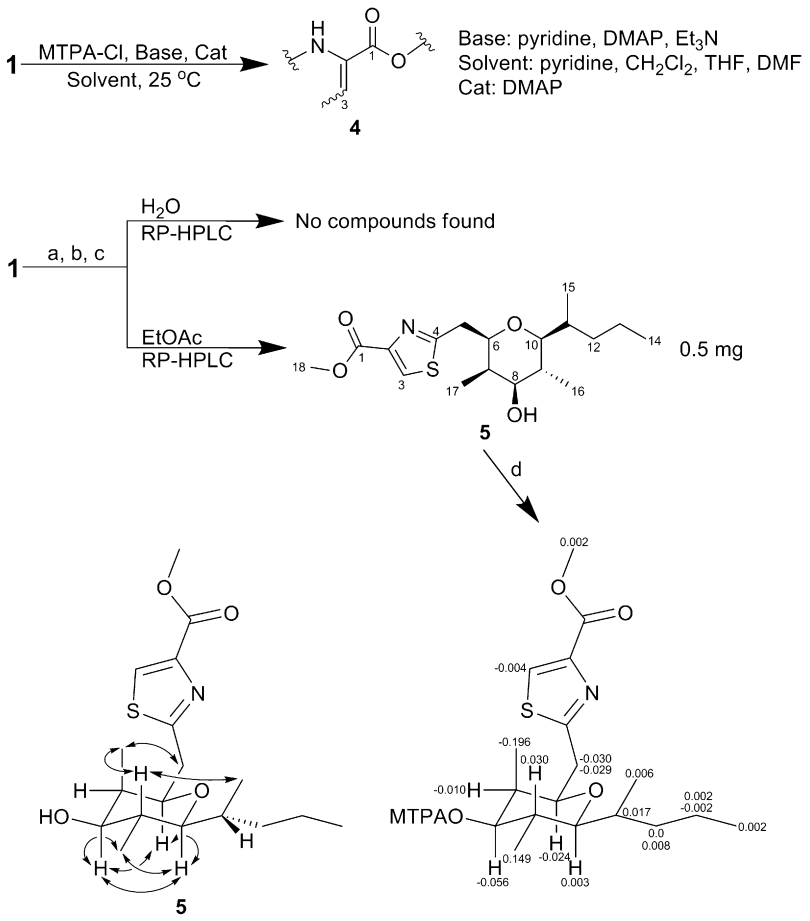

Figure 3. Chemical Degradation Efforts Used in Determining the Absolute Stereochemistry of Hoiamide A

Reagents and conditions: (a) 6M HCl, 110°C, 22 hr; (b) MeOH, $HCl_{(cat)}$, 25°C, 3 weeks; (c) solvent partitioning H_2O/EtOAc; and (d) MTPA, pyridine, DMAP, 25°C, 18 hr.

Dmetua residue. The diastereotopic methylene protons at δ3.22 (dd, *J* = 14.4, 10.2 Hz, H5b) and δ3.12 (dd, *J* = 14.4, 1.8 Hz, H5a) showed HMBC cross-peaks with carbons at δ169.2 (C4) in the thiazole ring, a methyl-bearing methine at δ39.2 (C7), and the oxygenated methine at δ77.5 (C6), which, in turn, was connected to another methine at δ83.2 (C10) through an ether linkage. This latter linkage was established on the basis of reciprocal HMBC correlations between their attached protons (H6/C10 and H10/C6). Moreover, this ether bridge formed a new six-membered heterocycle in derivative **5**, thereby satisfying the required 5 degrees of unsaturation. Additional 2D NMR data placed a 2-pentyl side chain on the carbon at δ83.2 (C10) and the final oxygenated methine at δ3.43 (H8) flanked by methyl-bearing methines at δ1.95 (H7) and δ1.68 (H9) to either side; each of the latter was connected to the bridged system described above. This analysis allowed assignment of the planar structure of derivative **5** (Figure 3), which likely results from the Dmetua residue via displacement of the methoxy group at C32 by the C36 hydroxy group with inversion of configuration (the absence of an epimer at C6 in **5** supports an S_N2 mechanism). (Neighboring group participation [anchimeric assistance] by the thiazole-ring sulfur lone pair might stabilize the protonated and thus positively charged oxygen atom of the leaving group [MeOH] via a five-membered ring intermediate, thus favoring an S_N2 nucleophilic substitution.)

Further NMR analysis of compound (**5**) provided insightful information on the relative configuration of Dmetua, which confirmed the assignments made by *J*-based configurational analysis. The highly shielded methyl doublet at δ0.96 (H17) was situated in an axial position, together with protons at δ3.70 (H6), δ3.43 (H8), δ1.68 (H9), and δ2.88 (H10), based on coupling constant information. Such an arrangement was consistent with NOESY data (Figure 3), which additionally defined the stereocenter at C11 outside the tetrahydropyran ring. The absolute stereochemistry at C8 was determined as *S* by the modified Mosher method (Ohtani et al., 1991), and with the relative configuration of **1** established via *J*-based analysis and of **5** by ^{1}H-^{1}H coupling constants and NOE data, the absolute stereochemistry of the Dmetua fragment could be assigned as 32*S*, 33*S*, 34*R*, 35*S*, 36*S*, and 37*R*. This completed the assignment of structure and stereochemistry of hoiamide A (**1**).

Hoiamide A (**1**) represents a particularly interesting example of a natural product deriving from a mixture of the polyketide synthase (PKS) and nonribosomal peptide synthetase (NRPS) pathways. The initial polyketide section, the Dmetua fragment, is unique to **1** and shows a typical remnant oxidation pattern at several sites, as well as methylation at the C-2 positions of predicted acetate units, which entirely derive from SAM methylation events in cyanobacteria. Excluding the branching carbons of the Dmetua moiety, the carbon chain is eleven carbons long and suggests either a propionate starter unit, the SAM methylation of an acetate starter, or a truncation of a hexaketide. Of these alternatives, we favor the SAM methylation possibility because (a) propionate is unknown as a starter unit in cyanobacterial polyketides (Grindberg et al., 2008), and (b) the remaining oxidations and methylations are positionally inconsistent with a terminal decarboxylation. Next, an intriguing tetrapeptide is created, with the three cysteine residues subject to heterocyclization reactions followed by dehydration. The first of these is further modified by oxidation to the thiazole ring, whereas the latter two are stereospecifically methylated at the alpha carbon, again, likely involving SAM as the methyl source. Cysteine-derived linear arrangements of 2,4-disubstituted thiazolines/thiazole rings possess a diverse

[a]Relative configuration and rotamer designation according to Matsumori et al. (1999).
[b]Weak couplings with $^3J_{H,H}$ < 0.5 Hz were considered as 0 Hz.
[c]No correlation observed in HSQMBC as expected for a coupling of 0 Hz.

Table 2. NMR Data for Derivative 5 in $CDCl_3$

Carbon	δ_C[a]	δ_H, multiplicity (Hz)[b]	COSY	HMBC (^1H to ^{13}C)	NOESY
1	161.6				
2	145.6				
3	127.8	8.09, s		1, 2, 4	
4	169.2				
5	37.7	a3.12, dd (14.4, 1.8)	6, 5b	4, 6, 7	17
		b3.22, dd (14.4, 10.2)	6, 5a	4, 6, 7	17
6	77.5	3.70, d (9.6)	5a, 5b, 7	4, 5, 8, 10, 17	8, 10
7	39.2	1.95, m	6, 8, 17	8, 9, 17	
8	76.7	3.43, dd (10.2, 4.8)	7, 9	9, 16, 17	6, 10, 16
9	33.9	1.68, m	8, 10, 16	8, 10	15, 17
10	83.2	2.88 dd (10.2, 1.8)	9, 11	6, 8, 11, 12, 15, 16	6, 8, 16
11	33.2	1.66, m	10, 15, 12a, 12b	12, 13, 15	14
12	37.1	a1.24, m	11, 12b	10, 11, 13, 14, 15	15
		b1.33, m	11, 12a	10, 11, 13, 14, 15	15
13	20.4	1.16, m	14	11, 12, 14	
14	14.4	0.79, t (7.2)	13	12, 13	11
15	13.1	0.87, d (7.2)	11	10, 11, 12	9, 12a, 12b
16	13.0	0.88, d (6.0)	9	8, 9, 10	8, 10
17	5.6	0.96, d (6.6)	7	6, 7, 8	5a, 5b, 9
18	52.5	3.95, s		1, 2	

[a] Recorded at 125 MHz.
[b] Recorded at 500 MHz.

range of biological activities (Carmeli et al., 1990, 1991, 1993; Naegeli and Zahner, 1980; Jansen et al., 1992) and are believed to play an important role in their mechanism of action (Wipf et al., 1998; Kwan et al., 2008). The fourth residue, isoleucine, is modified by a PKS extension, reduction of the ketone to an alcohol, and methylation of the acetate C-2 carbon. As a result of these tailoring reactions, this homologated Ile residue is chirally dense with four contiguous asymmetric centers. Next, a hydroxy acid common to many cyanobacterial natural products, hydroxyisovaleric acid (Hiva), is incorporated into hoiamide A (**1**). In the one other case where the gene structure for Hiva incorporation has been studied in a cyanobacterium—the natural product hectochlorin (Ramaswamy et al., 2007)—this occurs through initial activation of the α-keto acid and subsequent reduction to the hydroxy-acid once tethered to the NRPS condensation domain. Finally, the only amino acid in hoiamide A (**1**) not modified by a secondary tailoring reaction, L-threonine, is attached as the final residue. This terminating amino acid sequence, Thr-Hiva, has not been described in any other known cyanobacterial natural product. Finally, the C34 hydroxyl group in the Dmetua group is presumably involved in both hydrolysis from the NRPS as well as ester formation to the final 26-membered cyclic depsipeptide structure.

Hoiamide A: Pharmacological Studies

Hoiamide A Produces Sodium Influx in Neocortical Neurons

Systematic screening of natural product extracts, using a combination of high throughput Ca^{2+} and Na^+ influx assays in neocortical neurons, led to the identification of the novel bioactive cyclic peptide hoiamide A (**1**). Further characterization demonstrated that hoiamide A produced a rapid and concentration-dependent elevation of neuronal $[Na^+]_i$ in neocortical neurons as detected with the sodium-sensitive fluorescent dye, SBFI (Figure 4A). The concentration-response curve for hoiamide A-induced sodium influx was best fit by a three-parameter logistic equation yielding an EC_{50} value of 2.31 μM (95% confidence intervals [95% CI], 0.82–6.53) (Figure 4C). We and others have demonstrated that batrachotoxin is a full agonist at neurotoxin site 2 on the sodium channel α subunit (Cao et al., 2008; Catterall, 1977). We therefore compared the relative efficacies of hoiamide A and batrachotoxin as stimulators of neuronal $[Na^+]_i$. As shown in Figure 4B, batrachotoxin produced a rapid and concentration-dependent elevation of neuronal $[Na^+]_i$ with an EC_{50} value of 11.4 nM (95% CI, 6.92–18.8). The EC_{50} value for batrachotoxin-induced sodium influx is consistent with that reported by Cao et al. (2008). The maximum response for batrachotoxin-induced elevation of neuronal $[Na^+]_i$ was greater than 60 mM, whereas the maximal response for hoiamide A–induced increase in $[Na^+]_i$ was less than 20 mM. Nonlinear regression analysis of the hoiamide A concentration-response data revealed that the relative efficacy of hoiamide A for elevation of neuronal $[Na^+]_i$ was 0.38 (Figure 4C). These data are consistent with hoiamide A (**1**) acting as a partial agonist at neurotoxin site 2.

TTX Antagonizes Hoiamide A–Induced Elevation of Neuronal $[Na^+]_i$ in Neocortical Neurons

VGSCs and the *N*-methyl-D-aspartic acid (NMDA) and α-amino-3-hydroxyl-5-methyl-4-isoxazole-propionate (AMPA) subtypes of glutamate receptors represent the main routes for sodium influx in neocortical neurons. To further explore the mechanism of hoiamide A–induced sodium influx, we evaluated the effects

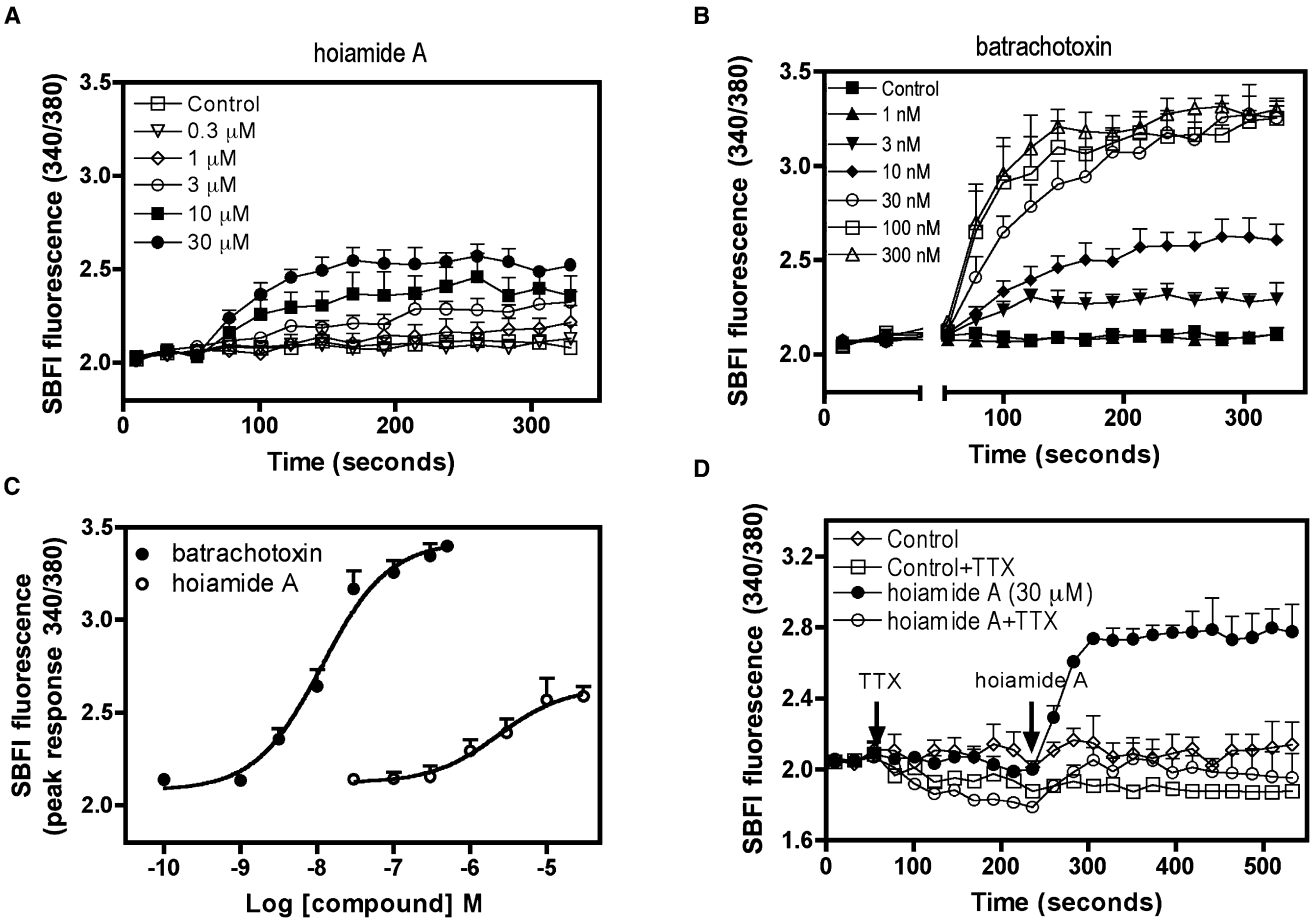

Figure 4. Hoiamide A Stimulates Na^+ Influx in Neocortical Neurons

(A) Time-response relationships for hoiamide A–induced elevation of neuronal $[Na^+]_i$ in neocortical neurons.

(B) Time-response relationships for batrachotoxin-induced elevation of neuronal $[Na^+]_i$ in neocortical neurons.

(C) Nonlinear regression analysis of the peak SBFI (340/380) response versus hoiamide A and batrachotoxin concentration.

(D) TTX inhibition of hoiamide A–induced elevation of neuronal $[Na^+]_i$. These data were obtained from at least three different cultures performed in duplicate.

of TTX (VGSC inhibitor), MK-801 (NMDA receptor antagonist), and NBQX (AMPA receptor antagonist) on hoiamide A–induced elevation of neuronal $[Na^+]_i$. Pretreatment with TTX (1 μM) eliminated the hoiamide A–induced elevation of neuronal $[Na^+]_i$ demonstrating the requirement for activation of VGSCs for hoiamide A (**1**)–induced sodium influx (Figure 4D). Pretreatment with MK-801 (1 μM) produced a partial, but statistically significant, decrease in hoiamide A–induced elevation of neuronal $[Na^+]_i$ (Figure S24A). This effect may be due to the engagement of NMDA receptors as a result of membrane depolarization, a consequence of activation of VGSCs. The AMPA receptor antagonist NBQX (5 μM) had no effect on hoiamide A–induced Na^+ influx (Figure S24B). Considered together, these data demonstrate that hoiamide A (**1**) is a VGSC activator.

Deltamethrin and PbTx-3 Enhancement of Hoiamide A–Induced Elevation of Neuronal $[Na^+]_i$ in Neocortical Neurons

Although the multiple neurotoxin sites on VGSCs are topologically distinct, there are strong allosteric interactions among them. Pyrethroids are synthetic insecticidal compounds that resemble natural pyrethrins (Lombet et al., 1988). Pyrethroids specifically bind to a site on the sodium channel α subunit that is distinct from neurotoxin site 1–6 and is allosterically coupled to sites 2, 3, and 5 (Trainer et al., 1993; Trainer et al., 1997). Therefore, to further explore the molecular mechanism of action for hoiamide A (**1**), we assessed the effect of a subthreshold concentration of deltamethrin (0.1 μM) on the hoiamide A–induced elevation of neuronal $[Na^+]_i$ in neocortical neurons. A concentration of deltamethrin (0.1 μM), which was inactive alone (Figure S25B), significantly increased the maximum response of hoiamide A–induced sodium influx from an AUC (fluorescence × min) value of 89.9 (95% CI, 81.5–98.2) to 141.4 (95% CI, 119.7–162.5) without altering the hoiamide A EC_{50} value (Figures 5A, 5C, and 5E). These data provide direct evidence that hoiamide A (**1**) binds to a site on the sodium channel that is allosterically coupled to the pyrethroid insecticide binding site. Brevetoxins are potent lipid-soluble polyether neurotoxins produced by the marine dinoflagellate, *Karenia brevis* (Baden, 1989). Brevetoxins interact specifically with neurotoxin site 5 on the α subunit of VGSC. Evidence for the allosteric coupling of neurotoxin site 2 and site 5 has been provided by demonstrating that

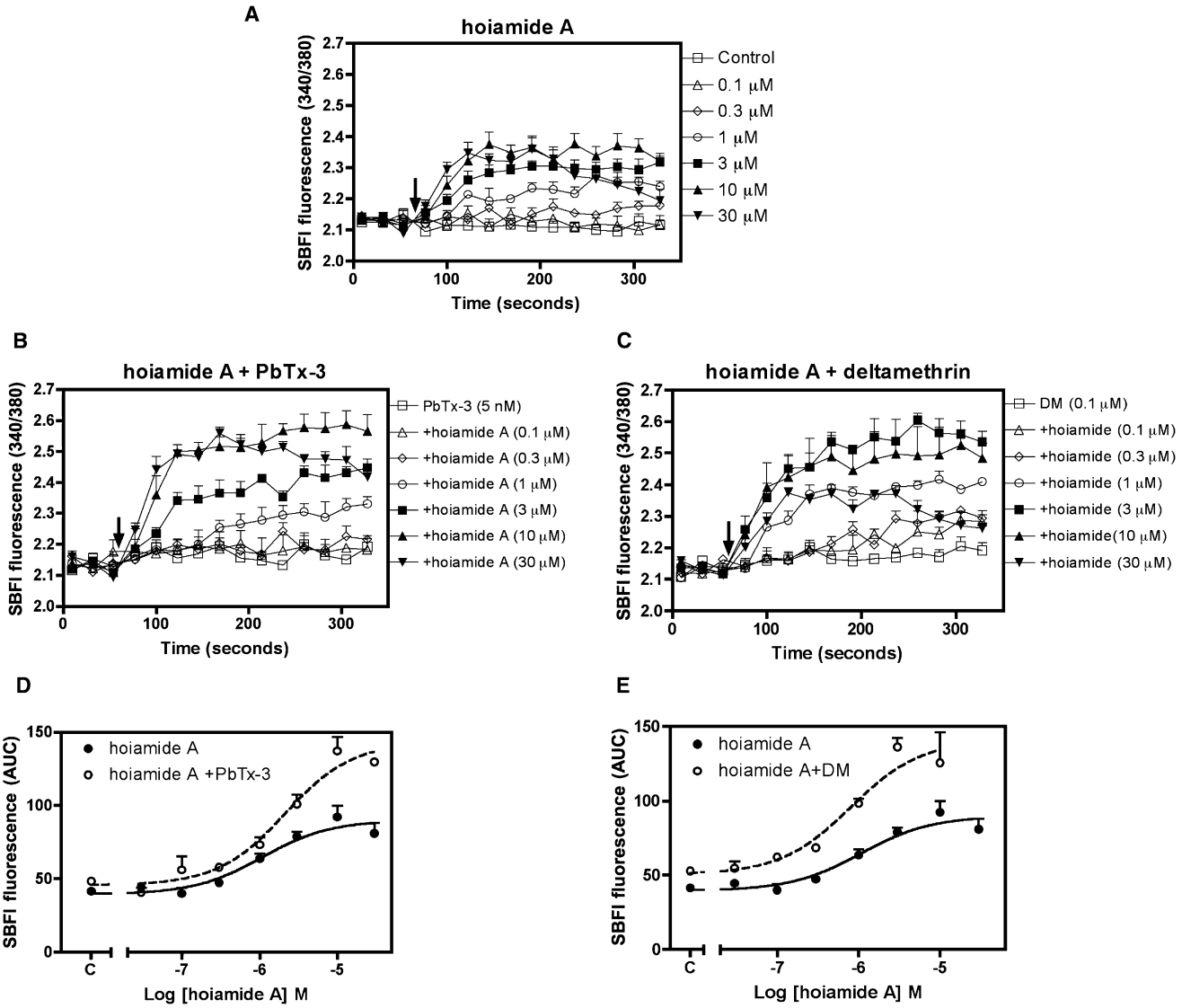

Figure 5. Deltamethrin (0.1 μM) and PbTx-3 (5 nM) Enhance Hoiamide A–Induced Elevation of Neuronal $[Na^+]_i$

(A) Time-response relationships for hoiamide A–induced elevation of neuronal $[Na^+]_i$.

(B) Time-response relationships for hoiamide A–induced elevation of neuronal $[Na^+]_i$ in the presence of 5 nM PbTx-3.

(C) Time-response relationships for hoiamide A–induced elevation of neuronal $[Na^+]_i$ in the presence of 0.1 μM deltamethrin.

(D) Nonlinear regression analysis of the SBFI response (area under the curve [AUC]) versus the concentration of hoiamide A in the presence and absence of 5 nM PbTx-3.

(E) Nonlinear regression analysis of the SBFI response (AUC) versus the concentration of hoiamide A in the presence and absence of 0.1 μM deltamethrin. Each data point represents the mean ± SEM from two experiments performed in triplicate.

the binding of [^{3}H]batrachotoxin to neurotoxin site 2 is enhanced by brevetoxins (Li et al., 2001; Sharkey et al., 1987). We therefore determined whether an allosteric interaction existed between site 5 and the hoiamide A (**1**) binding site. A concentration of brevetoxin 3 (PbTx-3, 5 nM), which was inactive alone (Figure S25A), also produced a significant increase in the maximum response of hoiamide A–induced sodium influx from an AUC (fluorescence × min) value of 89.9 (95% CI, 81.5–98.2) to 143.4 (95% CI, 129.7–157.4) with no corresponding effect on the hoiamide A EC_{50} value (Figures 5A, 5B, and 5D). These data suggest that a positive allosteric interaction exists between the hoiamide A (**1**) binding site and neurotoxin site 5 on VGSCs. These positive allosteric interactions between hoiamide A, and PbTx-3 and deltamethrin are therefore consistent with hoiamide A interacting with neurotoxin site 2.

Hoiamide A Inhibits the Specific Binding of [^{3}H]batrachotoxin A 20-α-benzoate ([^{3}H]BTX) to Neurotoxin Site 2 on VGSCs in Neocortical Neurons

[^{3}H]BTX is a radioligand probe that binds to neurotoxin site 2 on the VGSC α subunit (Catterall et al., 1981). This ligand interacts preferentially to the active or open conformation of the channel,

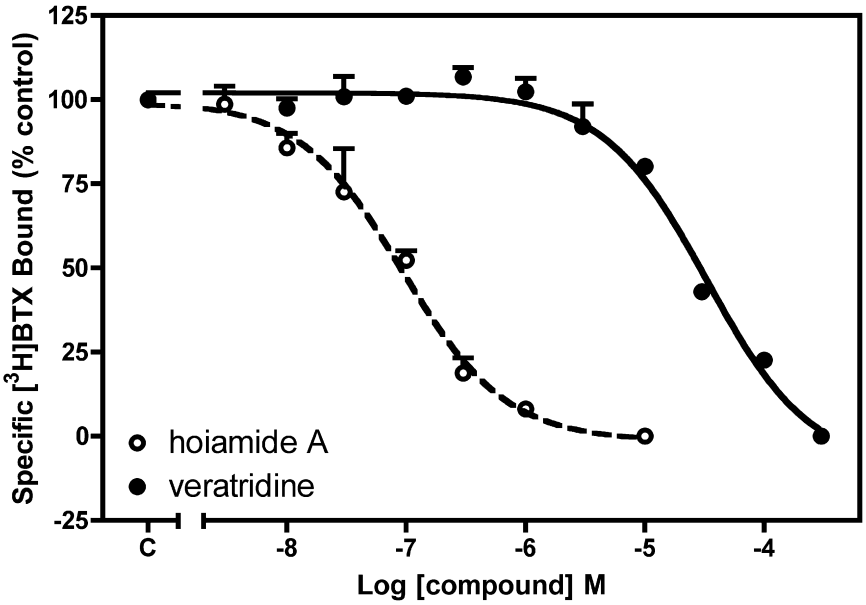

Figure 6. Hoiamide A and Veratridine Inhibit the Specific Binding of [^{3}H]BTX to VGSCs
Each data point represents the mean ± SEM from three experiments performed in triplicate.

and the specific binding is sensitive to conformational changes induced by the binding of neurotoxins at other sites on the sodium channel α subunit. We therefore used [^{3}H]BTX as a probe to provide further evidence for hoiamide A (**1**) interaction with neurotoxin site 2 on VGSCs. Inasmuch as the specific binding of [^{3}H]BTX is quite low in the absence of other sodium channel gating modifiers and is dramatically increased by the allosteric interaction of deltamethrin and brevetoxin, we assessed the influence of hoiamide A on [^{3}H]BTX binding in the presence of these allosteric modulators. As depicted in Figure 6, hoiamide A (**1**) produced a concentration-dependent inhibition of [^{3}H]BTX-specific binding in the presence of PbTx-3 (300 nM) and deltamethrin (10 μM). The hoiamide A IC_{50} value was 92.8 nM (95% CI, 56.6–152.1). The prototypic neurotoxin site 2 ligand veratridine also inhibited [^{3}H]BTX-specific binding to VGSCs with an IC_{50} value of 33.0 μM (95% CI, 24.2–45.1), indicating that it was much less potent than hoiamide A (Figure 6). Considered together, these data directly demonstrate that hoiamide A (**1**) interacts with neurotoxin site 2 on the VGSC α subunit.

Inhibition of BTX-Induced Increase in Neuronal [Na$^+$]$_i$ by Hoiamide A

We have previously demonstrated that saturating concentrations of neurotoxin site 2 ligands produce different maximal responses in sodium influx (Cao et al., 2008). We have demonstrated herein that hoiamide A (**1**) produced a maximum sodium influx that was less than that of the full agonist, batrachotoxin (Figure 4C). This suggests that hoiamide A acts as a partial agonist at neurotoxin site 2 on VGSCs. Catterall (1977) first demonstrated partial agonism at neurotoxin site 2 with a combination of a full activator (batrachotoxin) and a weak activator (aconitine). This interaction resulted in an inhibition of the response to the full activator by the weak activator. We have previously demonstrated that gambierol, a low-efficacy partial agonist at neurotoxin site 5, inhibited the full agonist PbTx-1-induced elevation of neuronal [Na$^+$]$_i$ (Cao et al., 2008). Thus, a low-efficacy agonist may act as a functional antagonist of a high-efficacy agonist at either neurotoxin site 2 or 5 on VGSCs (Cao et al., 2008). Given the modest efficacy of hoiamide A (**1**) as a stimulator of neuronal [Na$^+$]$_i$, we performed a titration with hoiamide A in the presence of a fixed concentration of the full agonist, batrachotoxin (30 nM). As depicted in Figure 7,

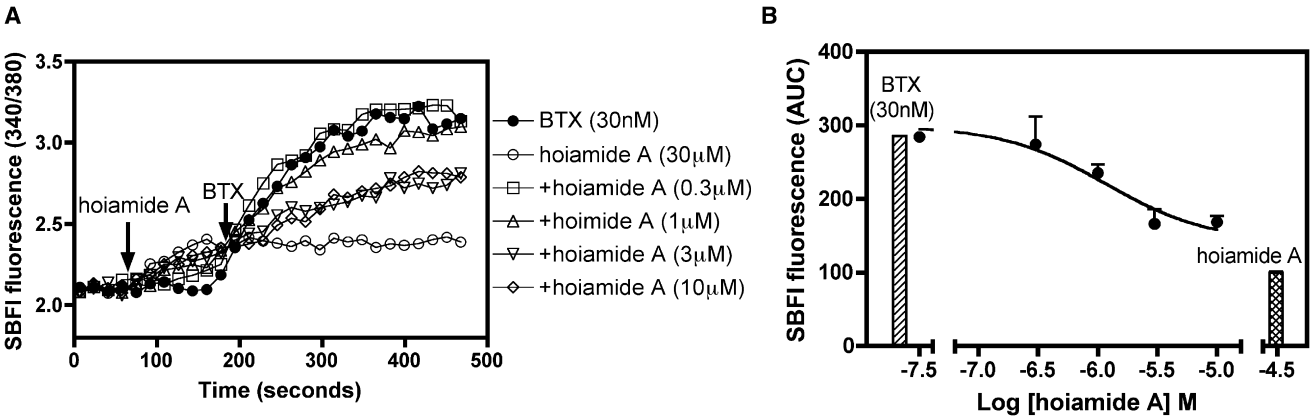

Figure 7. Hoamide A Titration in the Presence of a Saturating Concentration of the Full Agonist Batrachotoxin
(A) Time-response relationships for hoiamide A reversal of batrachotoxin (30 nM)–induced elevation of neuronal [Na$^+$]$_i$.
(B) Nonlinear regression analysis of the hoiamide A-induced reversal of the integrated SBFI response (AUC) to batrachotoxin (30 nM) in neocortical neurons. Histogram represents the responses to batrachotoxin (30 nM) and hoiamide A (30 μM) alone. These experiments were performed twice in triplicate with similar results.

the titration with hoiamide A produced a concentration-dependent reduction in batrachotoxin-induced sodium influx (SBFI AUC). These data demonstrate that hoiamide A (**1**) and batrachotoxin interact in a mutually exclusive manner with a common recognition site on VGSCs. The partial agonist activity of hoiamide A is therefore demonstrated by the ability of hoiamide A to produce a concentration-dependent inhibition of batrachotoxin-induced elevation of $[Na^+]_i$ in neocortical neurons.

SIGNIFICANCE

Marine cyanobacteria represent a particularly rich source of structurally diverse neurotoxic secondary metabolites, such as antillatoxin, kalkitoxin, and jamaicamide A (Grindberg et al., 2008). In the present study, we describe the isolation and structure elucidation of hoiamide A (1), a cyclic depsipeptide discovered in an environmental assemblage of *Lyngbya majuscula* and *Phormidium gracile*. Featuring three heavily modified regions (peptidic, triheterocyclic, and polyketide), hoiamide A (1) illustrates the intricate biosynthetic machinery responsible for the production of cyanobacterial compounds. Using a combination of neurochemical and pharmacological approaches, we have demonstrated that hoiamide A (1) represents a new chemotype to exhibit partial agonism at the neurotoxin site 2 on VGSCs. VGSCs are vital for central nervous system function. We and others have shown that an array of sodium channel gating modifiers produce $[Na^+]_i$ increments that are of sufficient magnitude to increase NMDA receptor channel activity (Cao et al., 2008; Yu and Salter, 1998; Yu and Salter, 1999). Sodium channel activators therefore appear capable of mimicking activity-dependent control of neuronal development by up-regulating NMDA receptor signaling pathways that influence neuronal growth and plasticity (George et al., 2009). VGSC activators may accordingly represent a novel pharmacologic strategy to regulate neuronal plasticity. Hoiamide A (1) therefore represents a structurally novel lead compound for drugs capable of promoting neuronal growth and plasticity.

EXPERIMENTAL PROCEDURES

See Supplemental Data for General Experimental Procedures and Analytical Data for Derivatives of Hoiamide A (**1**).

Collection of Biological Material

A composite collection of the marine cyanobacteria *Lyngbya majuscula* and *Phormidium gracile* (voucher specimen available from WHG as collection number PNG5-28-02-12) was obtained at a depth of 5–10 m from Hoia Bay, Papua New Guinea, in May 2002 (10° 15.990 S, 150° 46.169 E). Samples were stored in 70% EtOH at −20°C prior to extraction. Taxonomy was assigned by microscopic comparison with the description given by Komarek and Anagnostidis (2005), as well as Geitler (1932) (Supplemental Data).

Extraction and Isolation

Approximately 186 g (dry wt) of the cyanobacteria was extracted repeatedly with CH_2Cl_2/MeOH (2:1) to yield 4.377 g of crude extract. A portion of this material (3.5474 g) was fractionated by silica gel vacuum liquid chromatography using a stepwise gradient solvent system of increasing polarity starting from 10% EtOAc in hexanes to 100% MeOH, to produce nine fractions (A–I). The bioactive fraction F (0.7890 g) was subjected to a ^{1}H NMR-guided fractionation composed of two silica gel columns (60% and 50% EtOAc in hexanes, respectively) and reversed-phase HPLC (Phenomenex Jupiter 10 μ C18, 250 × 10 mm, 65% MeCN/H_2O with 0.1% TFA at 3 mL/min, detection at 210, 254 and 280 nm), to yield 150.0 mg of compound (**1**).

Hoiamide A (1): colorless amorphous solid; $[\alpha]^{23}_D$ +5 (*c* 5.5, $CHCl_3$); UV (MeCN) λ_{max} 250 nm (log ε 3.99); IR (neat) 3379, 2967, 2932, 2879, 1743, 1607, 1519, 1154, 1085, 735 cm^{-1}; for ^{1}H and ^{13}C NMR data, see Table 1; HR ESIMS *m/z* $[M+H]^+$ 926.4446 (calcd for $C_{44}H_{71}N_5O_{10}S_3$, 926.4441).

Neocortical Neuron Culture

Primary cultures of neocortical neurons were obtained from embryonic day 16 Swiss-Webster mice as described elsewhere (Cao et al., 2007). Briefly, pregnant mice were euthanized by CO_2 asphyxiation, and embryos were removed under sterile conditions. Neocortices were collected, stripped of meninges, minced by trituration with a Pasteur pipette, and treated with trypsin for 25 min at 37°C. The cells were then dissociated by two successive trituration and sedimentation steps in soybean trypsin inhibitor and DNase containing isolation buffer, centrifuged, and resuspended in Eagle's minimal essential medium with Earle's salt (MEM) and supplemented with 1 mM L-glutamine, 10% fetal bovine serum, 10% horse serum, 100 IU/ml penicillin, and 0.10 mg/ml streptomycin (pH 7.4). Cells were plated onto poly-L-lysine-coated 96-well (9 mm), clear-bottomed, black-well culture plates (Costar) at a density of 1.5 × 10^5 cells/well. Cells were then incubated at 37°C in a 5% CO_2 and 95% humidity atmosphere. Cytosine arabinoside (10 μM) was added to the culture medium on day 2 after plating to prevent proliferation of nonneuronal cells. The culture media was changed both on days 5 and 7 using a serum-free growth medium containing Neurobasal Medium supplemented with B-27, 100 IU/mL penicillin, 0.10 mg/mL streptomycin, and 0.2 mM L-glutamine. Neocortical cultures were used in experiments between 8–13 days in vitro (DIV). All animal use protocols were approved by the Institutional Animal Care and Use Committee (IACUC).

Intracellular Sodium Concentration ($[Na^+]_i$) Measurement

The neocortical neurons cultured in 96-well plates (DIV 8-13) were washed four times with Locke's buffer (8.6 mM HEPES, 5.6 mM KCl, 154 mM NaCl, 5.6 mM glucose, 1.0 mM $MgCl_2$, 2.3 mM $CaCl_2$, and 0.0001 mM glycine [pH 7.4]) using an automated cell washer (BioTeck Instrument Inc., VT, USA). The background fluorescence of each well was measured and averaged prior to dye loading. Cells were then incubated for 1 hr at 37°C with dye loading buffer (50 μL/well) containing 10 μM SBFI-AM and 0.02% Pluronic F-127. After 1 hr incubation in dye loading medium, cells were washed five times with Locke's buffer, leaving a final volume of 150 μl in each well. The plate was then transferred to the plate chamber of a FLEXstation™ II (Molecular Devices, Sunnyvale, CA, USA). Cells were excited at 340 nm and 380 nm and Na^+-bound SBFI emission was detected at 505 nm. Fluorescence readings were taken once every 5 s for 60 s to establish the baseline, and then 50 μl of neurotoxin containing solution (4×) was added to each well from the compound plate at the rate of 52 μL/s, yielding a final volume of 200 μL/well.

Whole Cell Binding Assay

At 8–10 days in culture, neocortical neurons cultured in 12-well plates were used for measurement of [^{3}H]BTX binding. Cells were first rinsed three times each with 1 ml of buffer A containing 140 mM choline chloride, 5 mM KCl, 1.8 mM $CaCl_2$, 0.8 mM $MgSO_4$, and 10 mM HEPES (pH 7.4 with 1 M Tris). Cells were then incubated with 0.5 ml of buffer B (buffer A plus 2 mg/mL BSA) containing 2 nM [^{3}H]BTX, 300 nM PbTx-3, 10 μM deltamethrin, and various concentrations of hoiamide A for 3–4 h. After incubation, cells were rinsed three times with 1 ml of buffer A before lysis with 500 μl of 1% Triton X-100 under a condition of constant shaking overnight. A 400 μl aliquot of the resulting lysate was collected, and [^{3}H]BTX bound was measured by liquid scintillation counter. Nonspecific binding of [^{3}H]BTX was determined as [^{3}H]BTX bound in the presence of 200 μM veratridine. Our preliminary results indicated that whole cell assays conducted at room temperature (22°C) provided an optimum signal-to-noise ratio; all binding experiments were conducted at 22°C.

Data Analysis

The raw emission data at each excitation wavelength were exported to an Excel work sheet and corrected for background fluorescence. The SBFI fluorescence ratios (340/380) versus time were then analyzed, and time-response and concentration-response graphs generated using Graphpad Prism

software (Graphpad Software Inc., San Diego, CA). The EC_{50} and maximum response values were determined by nonlinear regression analysis using a logistic equation.

SUPPLEMENTAL DATA

Supplemental Data include Supplemental Experimental Procedures and twenty-five figures and can be found with this article online at http://www.cell.com/chemistry-biology/supplemental/S1074-5521(09)00212-9.

ACKNOWLEDGMENTS

We thank D. Edwards and L. T. Simmons for collection of the assemblage of *L. majuscula* and *P. gracile* from Papua New Guinea, as well as A. Jansma and X. Huang for assistance with the Bruker 600 MHz TCI cryoprobe and Bruker 800 MHz NMR spectrometers, respectively. We appreciate N. Engene's input in the morphological characterization and taxonomic identification of the source organisms. Support of chemical and pharmacological aspects of the work was provided by NIH (NS053398).

Received: March 25, 2009
Revised: June 23, 2009
Accepted: June 26, 2009
Published: August 27, 2009

REFERENCES

Baden, D.G. (1989). Brevetoxins: unique polyether dinoflagellate toxins. FASEB J. *3*, 1807–1817.

Calmes, M., Escale, F., and Paolini, F. (1997). Viable use of 2-substituted thiazolidine-4-methanol diastereoisomeric mixtures during asymmetric borane reduction of aromatic ketones. Tetrahedron Asymmetry *8*, 3691–3697.

Cao, Z., George, J., Baden, D.G., and Murray, T.F. (2007). Brevetoxin-induced phosphorylation of Pyk2 and Src in murine neocortical neurons involves distinct signaling pathways. Brain Res. *1184*, 17–27.

Cao, Z., George, J., Gerwick, W.H., Baden, D.G., Rainier, J.D., and Murray, T.F. (2008). Influence of lipid-soluble gating modifier toxins on sodium influx in neocortical neurons. J. Pharmacol. Exp. Ther. *326*, 604–613.

Carmeli, S., Moore, R.E., Patterson, G.M.L., Corbett, T.H., and Valeriote, F.A. (1990). Tantazoles: unusual cytotoxic alkaloids from the blue-green alga *Scytonema mirabile*. J. Am. Chem. Soc. *112*, 8195–8197.

Carmeli, S., Paik, S., Moore, R.E., Patterson, G.M.L., and Yoshida, W.Y. (1993). Revised structures and biosynthetic studies of tantazoles A and B. Tetrahedron Lett. *34*, 6681–6684.

Carmeli, S., Moore, R.E., and Patterson, G.M.L. (1991). Mirabazoles, minor tantazole-related cytotoxins from the terrestrial blue-green alga *Scytonema mirabile*. Tetrahedron Lett. *32*, 2593–2596.

Catterall, W.A. (1977). Activation of the action potential Na^+ ionophore by neurotoxins. An allosteric model. J. Biol. Chem. *252*, 8669–8676.

Catterall, W.A., Morrow, C.S., Daly, J.W., and Brown, G.B. (1981). Binding of batrachotoxinin A 20-alpha-benzoate to a receptor site associated with sodium channels in synaptic nerve ending particles. J. Biol. Chem. *256*, 8922–8927.

Catterall, W.A., Cestele, S., Yarov-Yarovoy, V., Yu, F.H., Konoki, K., and Scheuer, T. (2007). Voltage-gated ion channels and gating modifier toxins. Toxicon *49*, 124–141.

Denac, H., Mevissen, M., and Scholtysik, G. (2000). Structure, function and pharmacology of voltage-gated sodium channels. Naunyn Schmiedebergs Arch. Pharmacol. *362*, 453–479.

Edwards, D.J., Marquez, B.L., Nogle, L.M., McPhail, K., Goeger, D.E., Roberts, M.A., and Gerwick, W.H. (2004). Structure and biosynthesis of the jamaicamides, new mixed polyketide-peptide neurotoxins from the marine cyanobacterium *Lyngbya majuscula*. Chem. Biol. *11*, 817–833.

Ersmark, K., Del Valle, J.R., and Hanessian, S. (2008). Chemistry and biology of the Aeruginosin family of serine protease inhibitors. Angew. Chem. Int. Ed. Engl. *47*, 1202–1223.

Fitch, C.P., Bishop, L.M., Boyd, W.L., Gortner, R.A., Rogers, C.F., and Tilden, J.E. (1934). "Water bloom" as a cause of poisoning in domestic animals. Cornell Vet. *24*, 30–39.

Geitler, L. (1932). Kryptogamen-flora von Deutschland, Osterreich und der Schweiz. In Cyanophyceae, L. Rabenhorst, ed. (Leipzig, Germany: Akademische Verlag;1985 reprint: Konigstein: Koeltz Scientific Books), pp. 1060–1061.

George, J., Dravid, S.M., Prakash, A., Xie, J., Peterson, J.H., Jabba, S.V., Baden, D., and Murray, T.F. (2009). Sodium channel activation augments NMDA receptor function and promotes neurite outgrowth in immature cerebrocortical neurons. J. Neurosci. *29*, 3288–3301.

Griesinger, C., Sorensen, O.W., and Ernst, R.R. (1987). Practical aspects of the E.COSY technique. Measurement of scalar spin-spin coupling constants in peptides. J. Magn. Reson. *75*, 474–492.

Grindberg, R.V., Shuman, C.F., Sorrels, C.M., Wingerd, J., and Gerwick, W.H. (2008). Neurotoxic alkaloids from cyanobacteria. In Modern Alkaloids, Structure, Isolation, Synthesis and Biology, E. Fattorusso and O. Taglialatela-Scafati, eds. (Weinheim, Germany: Wiley-VCH Verlang GmbH), pp. 139–170.

Jansen, R., Kunze, B., Reichenbach, H., Jurkiewicz, E., Hunsmann, G., and Hofle, G. (1992). Antibiotics from gliding bacteria XLVII. Thiangazole: a novel inhibitor of HIV-1 from *Polyangium* sp. Liebigs Ann. Chem. 357–359.

Komarek, J., and Anagnostidis, K. (2005). Cyanoprokaryota. In Susswasserflora von mitteleuropa, *vol 19/2*, B. Budel, L. Krienitz, G. Gartner, and M. Schagerl, eds. (Munchen, Germany: Elsevier GmbH), pp. 441–625.

Kwan, J.C., Rocca, J.R., Abboud, K.A., Paul, V.J., and Luesch, H. (2008). Total structure determination of grassypeptolide, a new marine cyanobacterial cytotoxin. Org. Lett. *10*, 789–792.

Li, W.I., Berman, F.W., Okino, T., Yokokawa, F., Shioiri, T., Gerwick, W.H., and Murray, T.F. (2001). Antillatoxin is a marine cyanobacterial toxin that potently activates voltage-gated sodium channels. Proc. Natl. Acad. Sci. USA *98*, 7599–7604.

Lombet, A., Mourre, C., and Lazdunski, M. (1988). Interaction of insecticides of the pyrethroid family with specific binding sites on the voltage-dependent sodium channel from mammalian brain. Brain Res. *459*, 44–53.

Luesch, H., Moore, R.E., Paul, V.J., Mooberry, S.L., and Corbett, T.H. (2001a). Isolation of Dolastatin 10 from the marine cyanobacterium *Symploca* species VP642 and total stereochemistry and biological evaluation of its analogue Symplostatin 1. J. Nat. Prod. *64*, 907–910.

Luesch, H., Yoshida, W.Y., Moore, R.E., Paul, V.J., and Corbett, T.H. (2001b). Total structure determination of apratoxin A, a potent novel cytotoxin from the marine cyanobacterium *Lyngbya majuscula*. J. Am. Chem. Soc. *123*, 5418–5423.

Marfey, P. (1984). Determination of D-amino acids. II. Use of a bifunctional reagent 1,5-difluoro-2,4-dinitrobenzene. Carlsberg Res. Commun. *49*, 591–596.

Marner, F.J., Moore, R.E., Hirotsu, K., and Clardy, J. (1977). Majusculamides A and B, two epimeric lipodipeptides from *Lyngbya majuscula* Gomont. J. Org. Chem. *42*, 2815–2819.

Marquez, B.L., Gerwick, W.H., and Williamson, R.T. (2001). Survey of NMR experiments for the determination of ^nJ(C,H) heteronuclear coupling constants in small molecules. Magn. Reson. Chem. *39*, 499–530.

Matsumori, N., Kaneno, D., Murata, M., Nakamura, H., and Tachibana, K. (1999). Stereochemical determinations of acyclic structures based on carbon-proton spin-coupling constants. A method of configuration analysis for natural products. J. Org. Chem. *64*, 866–876.

Moore, B.S. (2005). Biosynthesis of marine natural products: Microorganisms (Part A). Nat. Prod. Rep. *22*, 580–593.

Naegeli, H.U., and Zahner, H. (1980). Metabolites of microorganisms. Part 193. Ferrithiocin. Helv. Chim. Acta *63*, 1400–1406.

Ohtani, I., Kusumi, T., Kashman, Y., and Kakisawa, H. (1991). High-field FT NMR application of Mosher's method. The absolute configurations of marine terpenoids. J. Am. Chem. Soc. *113*, 4092–4096.

Paul, V.J., Arthur, K.E., Ritson-Williams, R., Ross, C., and Sharp, K. (2007). Chemical defenses: from compounds to communities. Biol. Bull. *213*, 226–251.

Pattenden, G., Thom, S.M., and Jones, M.F. (1993). Enantioselective synthesis of 2-alkyl substituted cysteines. Tetrahedron *49*, 2131–2138.

Pettit, G.R., Kamano, Y., Herald, C.L., Tuinman, A.A., Boettner, F.E., Kizu, H., Schmidt, J.M., Baczynskyj, L., Tomer, K.B., and Bontems, R.J. (1987). The isolation and structure of a remarkable marine animal antineoplastic constituent: Dolastatin 10. J. Am. Chem. Soc. *109*, 6883–6885.

Plaza, A., and Bewley, C.A. (2006). Largamides A-H, unusual cyclic peptides from the marine cyanobacterium *Oscillatoria* sp. J. Org. Chem. *71*, 6898–6907.

Ramaswamy, A.V., Flatt, P.M., Edwards, D.J., Simmons, T.L., Han, B., and Gerwick, W.H. (2006). The secondary metabolites and biosynthetic gene clusters of marine cyanobacteria. Applications in biotechnology. Front. Mar. Biotech. 175–224.

Ramaswamy, A.V., Sorrels, C.S., and Gerwick, W.H. (2007). Cloning and biochemical characterization of the hectochlorin biosynthetic gene cluster from the marine cyanobacterium *Lyngbya majuscula*. J. Nat. Prod. *70*, 1977–1986.

Rinehart, K.L., Kishore, V., Bible, K.C., Sakai, R., Sullins, D.W., and Li, K. (1988). Didemnins and tunichlorin: novel natural products from the marine tunicate *Trididemnum solidum*. J. Nat. Prod. *51*, 1–21.

Sharkey, R.G., Jover, E., Couraud, F., Baden, D.G., and Catterall, W.A. (1987). Allosteric modulation of neurotoxin binding to voltage-sensitive sodium channels by *Ptychodiscus brevis* toxin 2. Mol. Pharmacol. *31*, 273–278.

Sielaff, H., Christiansen, G., and Schwecke, R. (2006). Natural products from cyanobacteria: Exploiting a new source for drug discovery. IDrugs *9*, 119–127.

Sivonen, K., and Borner, T. (2008). Bioactive compounds produced by cyanobacteria. In Cyanobacteria, A. Herrero and E. Flores, eds. (Norwich, UK: Caister Acad. Press), pp. 159–197.

Tan, L.T. (2007). Bioactive natural products from marine cyanobacteria for drug discovery. Phytochemistry *68*, 954–979.

Taylor, C.P., and Meldrum, B.S. (1995). Na^+ channels as targets for neuroprotective drugs. Trends Pharmacol. Sci. *16*, 309–316.

Tidgewell, K., Clark, B.T., and Gerwick, W.H. (2009). The natural products chemistry of cyanobacteria. In Comprehensive natural products chemistry, 2nd ed. B. Moore and P. Crews, eds. (Oxford, UK: Elsevier Limited), in press.

Trainer, V.L., Moreau, E., Guedin, D., Baden, D.G., and Catterall, W.A. (1993). Neurotoxin binding and allosteric modulation at receptor sites 2 and 5 on purified and reconstituted rat brain sodium channels. J. Biol. Chem. *268*, 17114–17119.

Trainer, V.L., McPhee, J.C., Boutelet-Bochan, H., Baker, C., Scheuer, T., Babin, D., Demoute, J.P., Guedin, D., and Catterall, W.A. (1997). High affinity binding of pyrethroids to the alpha subunit of brain sodium channels. Mol. Pharmacol. *51*, 651–657.

Uhrin, D., and Barlow, P.N. (1997). Gradient-enhanced one-dimensional proton chemical-shift correlation with full sensitivity. J. Magn. Reson. *126*, 248–255.

Uhrin, D., Batta, G., Hruby, V.J., Barlow, P.N., and Kover, K.E. (1998). Sensitivity and gradient-enhanced hetero (ω_1) half-filtered TOCSY experiment for measuring long-range heteronuclear coupling constants. J. Magn. Reson. *130*, 155–161.

Van Wagoner, R.M., Drummond, A.K., and Wright, J.L.C. (2007). Biogenetic diversity of cyanobacterial metabolites. Adv. Appl. Microbiol. *61*, 89–217.

Williamson, R.T., Marquez, B.L., Gerwick, W.H., and Kover, K.E. (2000). One- and two-dimensional gradient-selected HSQMBC NMR experiments for the efficient analysis of long-range heteronuclear coupling constants. Magn. Reson. Chem. *38*, 265–273.

Williamson, R.T., Boulanger, A., Vulpanovici, A., Roberts, M.A., and Gerwick, W.H. (2002). Structure and absolute stereochemistry of phormidolide, a new toxic metabolite from the cyanobacterium *Phormidium* sp. J. Org. Chem. *67*, 7927–7936.

Wipf, P., Fritch, P.C., Geib, S.J., and Sefler, A.M. (1998). Conformational studies and structure-activity analysis of lissoclinamide 7 and related cyclopeptide alkaloids. J. Am. Chem. Soc. *120*, 4105–4112.

Wu, M., Okino, T., Nogle, L.M., Marquez, B.L., Williamson, R.T., Sitachitta, N., Berman, F.W., Murray, T.F., McGough, K., Jacobs, R., et al. (2000). Structure, synthesis, and biological properties of kalkitoxin, a novel neurotoxin from the marine cyanobacterium *Lyngbya majuscula*. J. Am. Chem. Soc. *122*, 12041–12042.

Yu, X.M., and Salter, M.W. (1998). Gain control of NMDA-receptor currents by intracellular sodium. Nature *396*, 469–474.

Yu, X.M., and Salter, M.W. (1999). Src, a molecular switch governing gain control of synaptic transmission mediated by *N*-methyl-D-aspartate receptors. Proc. Natl. Acad. Sci. USA *96*, 7697–7704.

